Full text open access online (Since 2001)

PRINT: ISSN 0972-3757 ONLINE: ISSN 2456-6330
Int J Hum Genet, 25(3): 177-194 (2025)
DOI: 10.31901/24566330.2025/25.03.923

Integrated Gene Ontology, Cheminformatics and Molecular Simulation Approaches for Elucidating the *MET/NFKB1/ABCG2* Inhibition by *Rheum emodi* Against Rheumatoid Arthritis

Xiaoqing Niu[1] and Yahong Fan[2*]

[1,2]The Eighth Department of Rheumatology, Xi'an Fifth Hospital/Shaanxi Integrated Traditional Chinese and Western Medicine Hospital, Xi'an, 710000, China

KEYWORDS Bioinformatics. Phytochemicals. Hub Genes. Protein-Protein Interaction. Apoptosis. qRT-PCR

ABSTRACT This study comprehensively investigated the bioactive compounds of *Rheum emodi* and their potential therapeutic impact on rheumatoid arthritis (RA). Initial screening identified six unique compounds with favourable drug-likeness, which collectively targeted 320 proteins. Network analysis revealed 27 gene overlaps with RA, highlighting five hub genes (MET, NFKB1, ABCG2, PARP1, ABCB1), wherein MET, NFKB1, and PARP1 were significantly upregulated in RA. Pathway enrichment analysis implicated these genes in lipid transport, cell communication, and key signa;ling pathways (NF-kappa B, PI3K-Akt, ABC transporters). Molecular docking and dynamics simulations indicated emodin exhibited strong, stable binding to MET and ABCG2 hubs. In vitro, *R. emodi* extract inhibited SW-982 cell viability (IC_{50} = 21.1/ µg/mL), induced apoptosis and ROS, and reduced cell migration. qRT-PCR confirmed downregulation of MET and NFKB1 post-treatment. Collectively, the findings support multi-target inhibitory actions of *R. emodi* extract in RA, underpinned by gene, pathway, and cellular effects.

INTRODUCTION

RA is a chronic, systemic autoimmune condition that mostly impacts synovial joints, resulting in pain, inflammation, and gradual joint deterioration (Finckh et al. 2022). The pathogenesis of rheumatoid arthritis is complex, including a sophisticated array of immune-mediated reactions that promote inflammation and tissue damage (Weyand and Goronzy 2021). Current therapeutic options, such as nonsteroidal anti-inflammatory drugs (NSAIDs) and disease-modifying antirheumatic drugs (DMARDs), have proven effective in alleviating RA symptoms and decelerating disease progression. However, these treatments frequently entail considerable adverse effects (Gadzhanova and Roughead 2024). This constraint has compelled the scientific community to investigate alternative treatment strategies, especially those originating from natural compounds with immunomodulatory and anti-inflammatory characteristics (Singh et al. 2020). *Rheum emodi*, often referred to as Indian rhubarb or "Dolu", has garnered significant interest for its traditional use in managing inflammatory disorders (Rolta et al. 2022). Indigenous to the Himalayan area, *Rheum emodi* has been used in ethnomedicine for the treatment of several ailments, such as gastrointestinal issues, hepatic problems, and inflammatory conditions (Rolta et al. 2022). The bioactive phytochemicals in *Rheum emodi*, particularly anthraquinones, tannins, and flavonoids, have substantial anti-inflammatory, antioxidant, and immunomodulatory effects, making the plant a prospective choice for rheumatoid arthritis therapy.

RA is characterised by the dysregulation of pro-inflammatory cytokines, which play a pivotal role in the inflammatory cascade of the illness (Kondo et al. 2021). The excessive production of these cytokines causes persistent synovial inflammation, resulting in joint degradation. Biologics designed to block these cytokines have shown therapeutic efficacy. Nevertheless, their extended usage may lead to immunosuppression and increased vulnerability to infections (Makuch et al. 2021). Thus, the investigation of phytochemicals that influence immunological pathways is a viable treatment option with reduced side effects. *Rheum emodi* has shown the ability to disrupt essential signalling pathways associated with inflammation, including the nuclear factor-kappa B (NF-κB) and mitogen-activated protein kinase (MAPK) pathways (Shen et al. 2022; Zhang et al. 2021). These pathways govern the synthesis of pro-inflammatory cytokines and are involved in the pathophys-

Address for correspondence:
Yahong Fan
E-mail: yohongfan@proton.me
<https://orcid.org/0009-0003-6498-7238>
*<https://orcid.org/0009-0005-1234-3371>

iology of rheumatoid arthritis. The bioactive components of *Rheum emodi* may function as multi-target medicines by altering various molecular pathways, providing a supplementary approach to traditional RA therapy.

Network pharmacology is an integrated, systems-oriented methodology that amalgamates bioinformatics, cheminformatics, and systems biology to elucidate the intricate connections between pharmaceuticals and biological systems (Zhou et al. 2025). This technique is especially appropriate for examining the pharmacological characteristics of herbal remedies, which include several bioactive components with potential multi-target effects (Jiang et al. 2025). Network pharmacology facilitates the identification of crucial biological targets and pathways related to rheumatoid arthritis, enhancing the comprehension of the therapeutic benefits of *Rheum emodi*. Gene Ontology (GO) analysis offers a structured methodology for the annotation of genes and proteins according to their related biological processes, molecular activities, and cellular components (Chen et al. 2025). In rheumatoid arthritis, GO analysis clarifies the principal dysregulated biological processes, including cytokine-mediated signalling and immunological responses. By correlating the bioactive ingredients of *Rheum emodi* with these processes, investigators may anticipate the plant's potential therapeutic capabilities, elucidating how these compounds may modulate inflammatory pathways at the molecular level. Molecular docking is a computer method that simulates the binding interactions of small compounds and target proteins, providing insights into the molecular mechanisms of action (Stanzione et al. 2021). Docking studies of *Rheum emodi* can model the interactions between its bioactive components and critical proteins associated with rheumatoid arthritis. Molecular docking elucidates the potential mechanisms by which these drugs may limit the action of pro-inflammatory cytokines. Molecular dynamics (MD) simulations further validate by assessing the stability, and flexibility of compound-protein interactions over time under physiological settings (AlRawashdeh and Barakat 2023). MD simulations are especially valuable for comprehending the dynamic nature of these interactions, providing a more accurate representation of the compound's potential effectiveness. Single gene expression analysis facilitates the examination of certain genes involved in the development of an ailment and the influence of treatment drugs on their expression levels (Patel et al. 2020). This methodology delivers a concentrated and quantitative evaluation of the plant's anti-inflammatory properties at the molecular level, presenting concrete proof of its potential therapeutic advantages in rheumatoid arthritis.

The incorporation of *Rheum emodi* as a treatment for rheumatoid arthritis, examined using network pharmacology methodologies, signifies a prospective study domain. The use of technologies including gene ontology analysis, molecular docking, molecular dynamics simulations, and single gene expression analysis facilitates a thorough comprehension of how the plant's bioactive chemicals influence critical molecular pathways associated with rheumatoid arthritis. These sophisticated approaches not only enhance the understanding of the pharmacological attributes of *Rheum emodi* but also facilitate the creation of innovative, multi-targeted therapeutics with less adverse effects relative to traditional treatments for rheumatoid arthritis.

Objectives

This investigation endeavours to rigorously elucidate the pharmacotherapeutic efficacy of *Rheum emodi* bioactive constituents in mitigating RA through an integrative paradigm synthesising phytochemical screening, network pharmacology, molecular dynamics, and transcriptomic profiling. Specific aims include discerning bioactive moieties with optimal pharmacodynamic attributes, delineating their proteomic interactions, and identifying genetic congruences with RA via network topological analysis to pinpoint pivotal hub-genes. The study further seeks to interrogate ontological enrichment in lipid translocation, intercellular signalling, and critical transduction pathways, evaluate molecular binding affinity and conformational stability to hub-genes through in silico docking and dynamics simulations, and substantiate in vitro bioactivity of *R. emodi* extract by assessing SW-982 cellular viability suppression, apoptosis induction, ROS elicitation, migration inhibition, and transcriptomic modulation via qRT-PCR to validate polypharmacological inhibitory mechanisms in RA.

MATERIAL AND METHODS

Sourcing and Screening

The *Rheum emodi* bioactive ingredients were obtained from the IMPPAT (https://cb.imsc.res.in/imppat/) and KNApSAcK (http://www.knapsackfamily. com/KNApSAcK/) databases (Shinbo et al. 2006; Vivek-Ananth et al. 2023). They were then subjected to screening on the SwissADME (https://www.swissadme.ch/) platform (Daina et al. 2017). The screening process included checking for bioavailability scores of 0.55 or above and making sure there were no drug-likeness rule violations by strictly adhering to drug-likeness requirements.

Rheum Emodi Bioactive Principles and Disease Targets

The SwissTarget Prediction (http://www.swisstargetprediction.ch/) and SuperPred (http://www.swisstargetprediction.ch/) platforms were used to find the biological targets of the bioactive chemicals from *Rheum emodi* (Daina et al. 2019). The probability score level was set at ≥ 0.10. Then, disease-related targets for rheumatoid arthritis were found in the GeneCards (https://www.genecards. org/) database by searching for "Rheumatoid Arthritis" (Stelzer et al. 2016).

Common Targets and String Generation

To accomplish overlapping, the ingredients and RA targets were submitted to Venny 2.0. Afterwards, PPI was built using the STRING (https://string-db.org/cgi/input?sessionId= bBcFTnU1RMRJ& input_page_ show_search= on) database, which allowed for the deletion of disconnected nodes and was configured for 3D string production (Szklarczyk et al. 2021).

Rheum emodi Targets Network and PPI Network Construction

After uploading the *Rheum emodi* target file to Cytoscape, the ingredients were assigned source nodes and the target genes were assigned target nodes. Through the cytohubba plugin, the researchers were able to see how the *Rheum emodi* principles interacted with one another and targets. In the same way, the researchers obtained the string data file in .tsv format, transformed it to Microsoft Excel, and then used Cytoscape to see the network. After that, the researchers conducted a degree-based network analysis in Cytoscape, which revealed five highly interacting hub genes.

Gene-Ontology and KEGG Enrichment

The gene ontology enrichment was analysed using ShinyGo 0.80 platform (http://bioinformatics. sdstate.edu/go/), which involved biological processes (BP), cellular component (CC) and molecular function (MF). The mechanisms that may be affected by using the bioactive principles from *Rheum emodi* could then be identified. Also, the platform was used to study KEGG enrichment, which mapped common target genes and enriched pathways.

Molecular Docking

The CB-Dock2 (https://cadd.labshare.cn/cb-dock2/index.php) web-based molecular docking program first found five CurPockets. After then, these CurPockets were coupled with the ligand using a blind docking technique. The RCSB PDB database was used to retrieve the receptor structures, whereas ChemBioDraw 3D Ultra 11.0 was used to construct the PDB structure of the ligand. In particular, the PDB IDs for MET is 3DKF, for NFKB1 is 8TQD, and for ABCG2 is 6VXH. By using BIOVIA Discovery Studio, the docking data were subjected to further analysis and visualisation for 2D interactions.

MD Simulations

The docked complexes were simulated molecularly utilising the iMODS (https://imods.iqf.csic.es/) and CABS-flex (https://biocomp.chem.uw.edu.pl/CABSflex2/about) platforms. iMODS performed Normal Mode Analysis (NMA) to evaluate flexibility using B-factor calculations and helped identify structural deformities (Kuriata et al. 2018; López-Blanco et al. 2014). Meanwhile, the CABS-flex platform provided additional insights on the complexes' contact maps and RMSFs in great detail. The docked complexes' molecular stiffness, flexibility, and stability were thoroughly assessed by both platforms.

Single Gene Expression Analysis

The researchers used the Rheumatoid Arthritis Bioinformatics Centre (RABC: http://www. one-third-lab.com/RABC/index.php/Index/index.html) platform to do single gene expression analysis, which allowed the researchers to identify hub gene expression in both healthy controls and RA patients. With 689 samples totalling 354 RA patients and 335 healthy controls, the RABC134 dataset provided strong evidence for comparing gene expression patterns.

Extract Preparation

R. emodi rhizomes were collected, thoroughly washed with distilled water, and air-dried at room temperature for 72 hours. The dried rhizomes were then finely ground using a mechanical grinder. Approximately 500g of the powdered material was extracted with an equal volume (1:1, v/v) of ethanol and dichloromethane. The mixture was continuously agitated at room temperature for 24 hours. After extraction, the solution was filtered through Whatman No. 1 filter paper and the solvents were evaporated under reduced pressure using a rotary evaporator at 40°C. The resulting crude extract was stored at –10°C until further use.

Cell Culture

SW-982 cells were cultured in Dulbecco's Modified Eagle Medium (DMEM) supplemented with 10 percent foetal bovine serum and 1 percent penicillin-streptomycin. Cells were maintained at 37°C in a humidified incubator with 5 percent CO_2. For experiments, cells were seeded in 96-well plates at a density of approximately 5,000 cells per well for the cytotoxicity assay and in 6-well plates for RNA isolation required in qRT-PCR studies. The cultures were allowed to reach 80 percent confluence before treatment.

Cytotoxicity Analysis

To evaluate cytotoxicity, SW-982 cells were exposed to a series of extract concentrations (0, 10, 20, 40, 80/ µg/mL) for 24 hours. Following treatment, 10/ µL of Cell Counting Kit-8 (Merck KGaA, Darmstadt, Germany) reagent was added to each well and the plates were incubated for an additional 2 hours at 37°C. Absorbance was measured at 450/ nm using a microplate reader. The percentage of viable cells was calculated relative to the untreated control, and dose-response curves were generated to determine the IC_{50} value.

DAPI Staining Assay for Apoptosis

SW-982 cells were seeded in 24-well plates and treated with ethanol/dichloromethane extract of *Rheum Emodi* at control (vehicle) and IC50 concentrations for 24 hours. After treatment, cells were fixed with 4 percent paraformaldehyde, permeabilised with 0.1 percent Triton X-100, and stained with DAPI (1 µg/mL) for 15 minutes in the dark. Nuclear morphology was examined under a fluorescence microscope to qualitatively assess apoptotic features such as chromatin condensation and nuclear fragmentation. Representative images were captured for each treatment group.

DCFDA Assay for ROS Detection

SW-982 cells were incubated with 10 µM DCFDA for 30 minutes at 37°C after treatment with *Rheum emodi* extract (control and IC50). Cells were washed with PBS, and fluorescence intensity was visualised under a fluorescence microscope. The presence and relative intensity of green fluorescence (indicative of ROS production) were qualitatively compared between treatment groups. Representative images were documented to demonstrate differences in ROS levels.

Scratch Assay for Cell Migration

SW-982 cells were grown to confluence in 6-well plates, and a scratch was made using a sterile pipette tip. Cells were treated with *Rheum emodi* extract (control and IC50) and monitored for 24 hours. Images were captured at 0, 12, and 24 hours to qualitatively assess cell migration into the scratch area. The extent of wound closure was visually compared between treatment groups, with representative images taken to illustrate differences in migratory behaviour.

qRT-PCR Analysis

Total RNA was then isolated using a commercial extraction kit (TRIzol reagent, Thermo Fisher

Scientific), and the quality and concentration of RNA were assessed spectrophotometrically. One microgram of RNA was reverse-transcribed into cDNA using a reverse transcription kit (OriGene Technologies, Inc. Rockville, USA). Quantitative real-time PCR (qRT-PCR) was performed using SYBR Green PCR Master Mix (Bio-Rad, USA) for MET, NFKB1, and ABCG2, with GAPDH serving as the internal control. Each reaction was set up in triplicate, and the amplification protocol followed standard cycling conditions. Relative gene expression was quantified using the $2^{-\Delta\Delta Ct}$ method, comparing treated samples to untreated controls. Table 1 represents the RNA primer sequence for MET, NFKB1 and ABCG2.

RESULTS

Bioactive Ingredients Identified and Screened

A total of 26 bioactive ingredients were obtained from the IMPPAT database and 20 from KNAPSACK for *Rheum emodi*. Upon the elimination of duplicates, 32 distinct compounds remained. Subsequently, a SwissADME analysis was performed, resulting in the exclusion of 24 compounds owing to a bioavailability score lower than 0.55 and violations of Lipinski's Rule of Five (Fig. 1A). Aloe emodin and catechin were identified as isomers among the remaining compounds, resulting in a final collection of 6 unique compounds (Table 2) for further examination.

Number and Targets Identified for Compounds and RA

The six compounds exhibited a total of 503 targets, with 500 identified by SwissTarget Prediction (Fig. 1B-F) and 3 confirmed targets for (-)-epicatechin using SuperPred. After the removal of 183 duplicate targets, 320 targets remained. Applying a probability filter of 0.10 resulted in 36 genes that retained (Table 3). A network visualisation was performed on the compounds and their targets to represent the maximum number of targets per compound remaining after applying the criteria (Fig. 2). It showed 39 nodes and 42 edges, with emodin exhibiting the most interactions, linked to 32 nodes and 33 edges. The search for RA related targets on GeneCards discovered 6,786 disease unique targets.

Construction of Networks

The Venny 2.0 analysis identified 27 overlapping gene targets between the bioactive components of *Rheum emodi* and RA, as seen in Table 3 and Fig. 3A. The 27 genes were then uploaded to the STRING database to evaluate PPI and to create the interaction network (Fig. 3B), after which isolated nodes were eliminated. The network file created by STRING was subsequently downloaded and visualised using Cytoscape, displaying 24 nodes and 116 edges (Fig. 3C). Based on the degree-method within the Cytohubba plugin in Cytoscape, five principal hub genes were discovered from this network, namely, MET, NFKB1, ABCG2, PARP1, and ABCB1 (Fig. 3D).

Pathways Enrichment Analysis with GO and KEGG

The outcomes of the GO enrichment analysis revealed significant BP involved in lipid transport, cellular response to lipids and organic cyclic compounds, cell differentiation, and positive regulation of signalling, cell communication, and molecular function (Fig. 4A). Key CC identified include the external side of the apical plasma membrane (Fig. 4B). In terms of MF, the analysis highlighted activities related to transmembrane receptor protein tyrosine kinase, protein kinase activity, and various binding interactions, including ATP, nucleotide, and small molecule binding (Fig. 4C). The KEGG pathway analysis further identified several critical signalling pathways, including ABC transporters, NF-kappa B signalling, PI3K-Akt signalling, EGFR tyrosine kinase inhibitor resistance, B-cell receptor signalling, and pathways involved in

Table 1: The RNA primer sequence

Gene	*Forward sequence*	*Reverse sequence*
MET	TGCACAGTTGGTCCTGCCATGA	CAGCCATAGGACCGTATTTCGG
NFKB1	GCAGCACTACTTCTTGACCACC	TCTGCTCCTGAGCATTGACGTC
ABCG2	GTTCTCAGCAGCTCTTCGGCTT	TCCTCCAGACACACCACGGATA

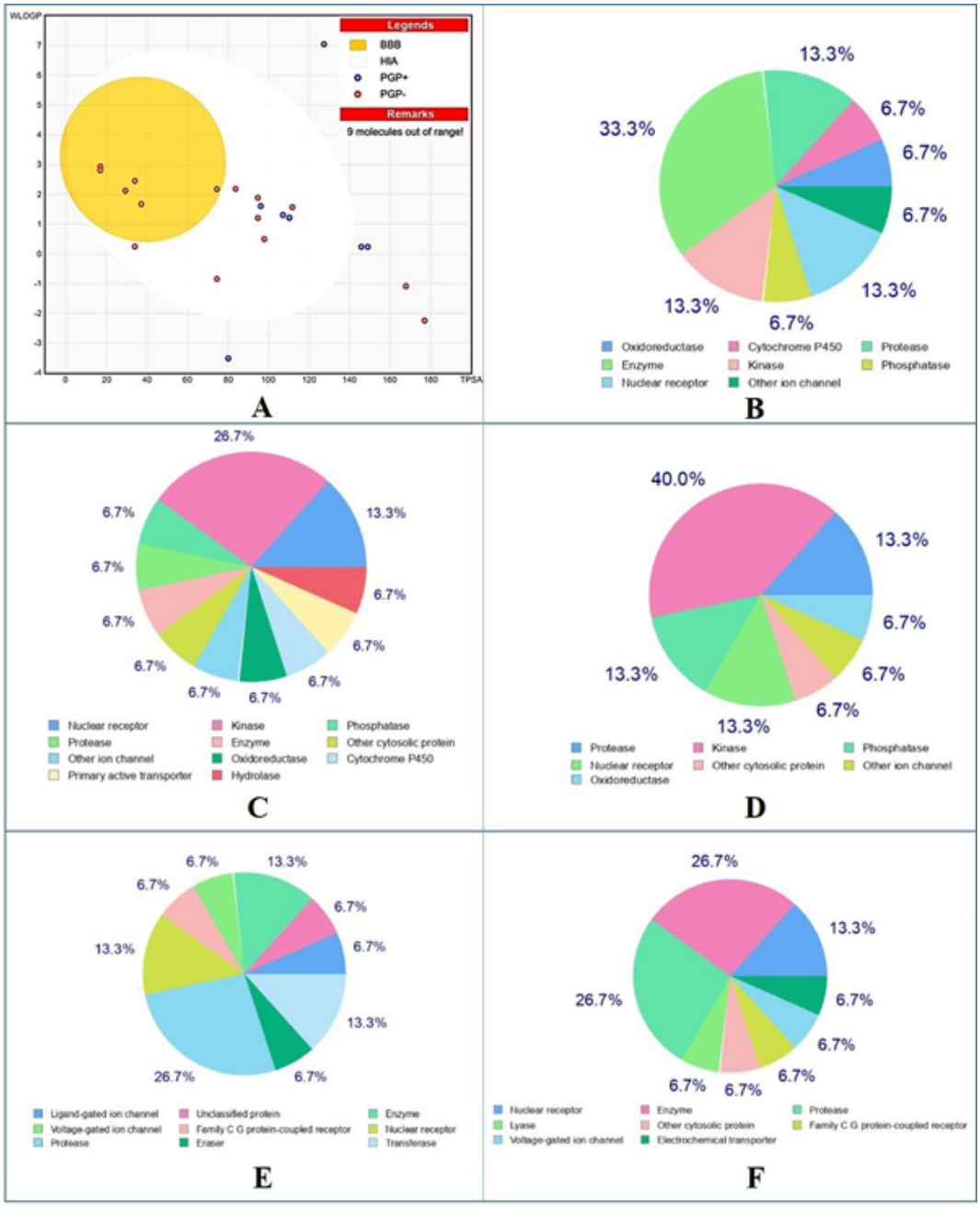

Fig. 1. (A) The BOILED-Egg model assessment of 32 bioactive compounds derived from *Rheum emodi*, evaluating their bioavailability and drug-likeness. The model categorises compounds based on their predicted gastrointestinal absorption and blood-brain barrier permeability

Table 2: Bioactive ingredients surviving screening criteria for bioavailability and drug likeness violations from Rheum emodi

Molecule	*Structure*	*Formula*	*MW*	*Bioavailability Score*	*Identifier*
Rhein	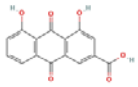	C15H8O6	284.22	0.56	IMPHY002157
Emodin	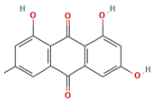	C15H10O5	270.24	0.55	IMPHY011543
Physcion	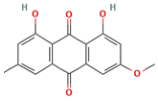	C16H12O5	284.26	0.55	IMPHY012117
(-)-Epicatechin	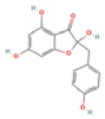	C15H14O6	290.27	0.55	C00000956
Maesopsin	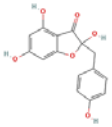	C15H12O6	288.25	0.55	C00008066
Carpusin	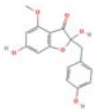	C16H14O6	302.28	0.55	C00008067

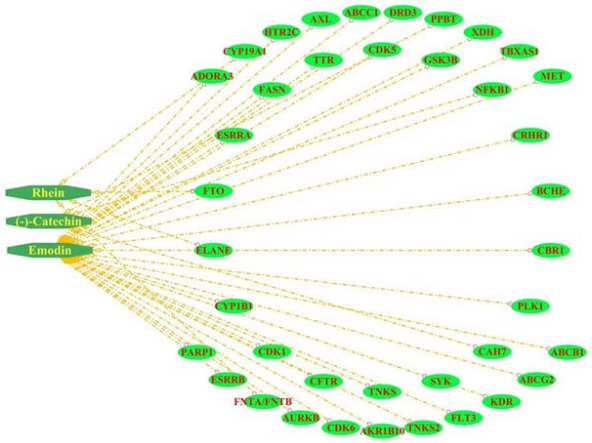

Fig. 2. Compound-Target Interaction Network revealing high interaction for emodin with 32 nodes and 33 edges

Table 3: Common genes overlapping in compound targets and RA

S. No.	*Gene symbol*	*S. No.*	*Gene symbol*
1.	FTO	2.	CRHR1
3.	CYP19A1	4.	DRD3
5.	ELANE	6.	CDK6
7.	ABCB1	8.	ABCG2
9.	BCHE	10.	HTR2C
11.	XDH	12.	ESRRA
13.	ADORA3	14.	ESRRB
15.	KDR	16.	FLT3
17.	PLK1	18.	SYK
19.	MET	20.	GSK3B
21.	AXL	22.	ABCC1
23.	FASN	24.	TTR
25.	PARP1	26.	CFTR
27.	NFKB1		

cancer, hepatitis C, hepatocellular carcinoma, and focal adhesion, underscoring the involvement of *Rheum emodi* bioactive compounds in diverse molecular mechanisms associated with RA and related diseases (Fig. 4D). Further gene mapping was performed to the overlapping genes in the enriched pathways including NFKB signalling and B cell receptor signalling pathway as shown in Fig. 5A and 5B, respectively.

Molecular Docking Insights for Top Three Hub Genes

The molecular docking results for emodin against MET, NFKB1, and ABCG2 demonstrated notable binding affinities and interactions (Table 4). For the Emodin-MET complex, a Vina score of -8.5 was observed within a CurPocket of 2845 Å^3, interacting with key residues such as ILE1084, ARG1086, and MET1211, suggesting a strong binding interaction (Fig. 6A). The Emodin-NFKB1 com-

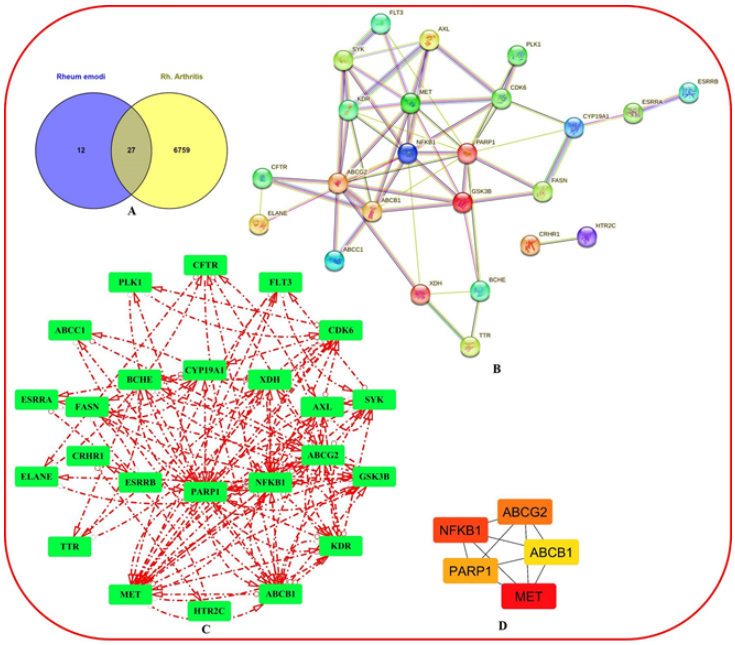

Fig. 3. Venn Plot and PPI Network:
(A) Venn diagram illustrating the overlapping gene targets between the bioactive compounds of *Rheum emodi* and rheumatoid arthritis
(B) STRING network showing the protein-protein interactions among these targets, highlighting their interconnectedness and potential collaborative roles in biological processes related to rheumatoid arthritis
(C) Protein-protein interaction network constructed using Cytoscape, displaying the relationships among the gene targets associated with the bioactive compounds of *Rheum emodi*
(D) The five hub genes identified within the network, namely, MET, NFKB1, ABCG2, PARP1, and ABCB1, emphasising their potential significance in mediating the therapeutic effects of the compounds in rheumatoid arthritis

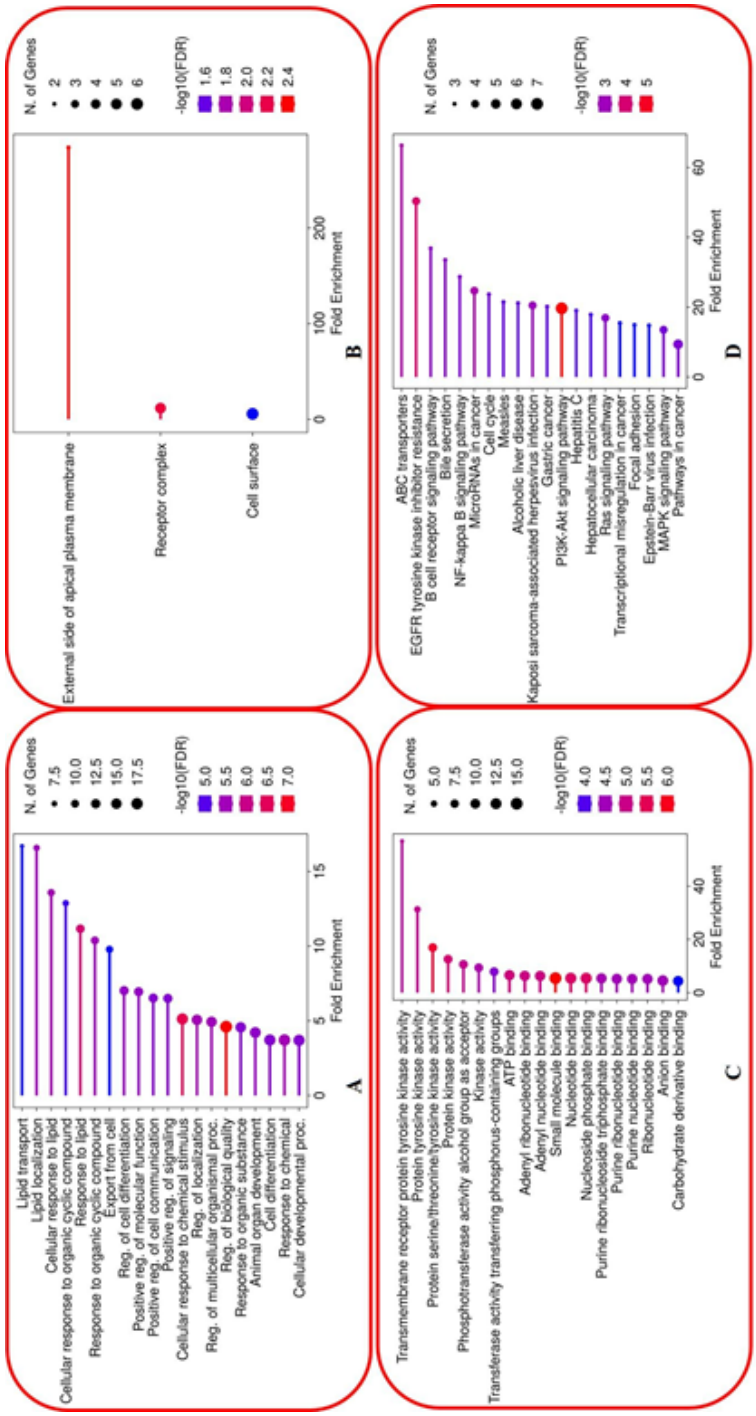

Fig. 4. (A) GO enrichment analysis revealing significant biological processes (BP) associated with lipid transport, cellular responses to lipids and organic cyclic compounds, cell differentiation, and positive regulation of signalling and molecular function (B) Identification of key CC highlighting the external side of the apical plasma membrane associated with the target genes (C) MF analysis showcasing activities related to transmembrane receptor protein tyrosine kinase, protein kinase activity, and various binding interactions, including ATP, nucleotide, and small molecule binding (D) KEGG pathway analysis illustrating critical signalling pathways associated with *Rheum emodi* bioactive compounds, including ABC transporters, NF-kappa B signalling, PI3K-Akt signalling, and pathways relevant to cancer, hepatitis C, and hepatocellular carcinoma

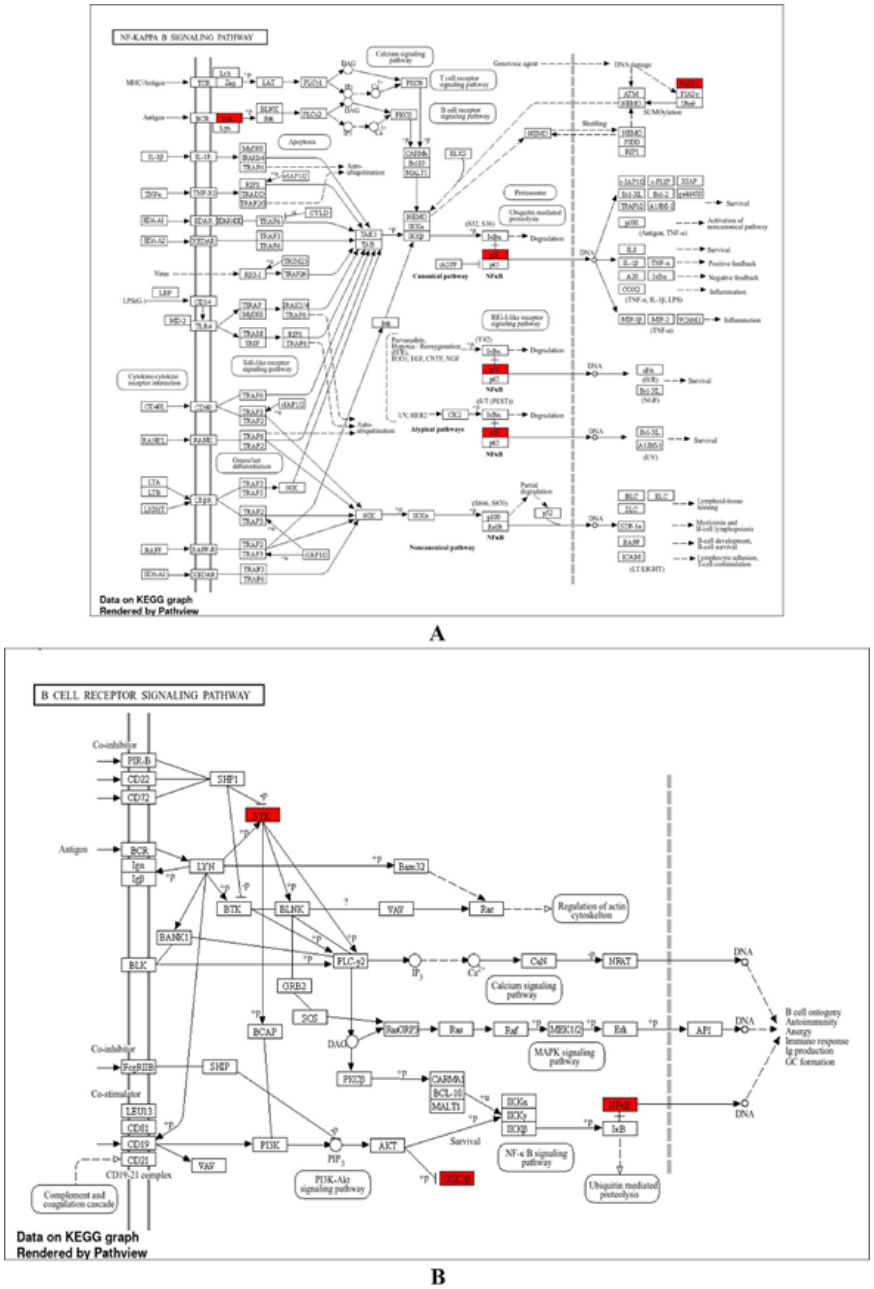

Fig. 5. (A) Gene mapping of overlapping genes within the enriched NFKB signalling pathway, highlighting their potential roles in rheumatoid arthritis
(B) Gene mapping of overlapping genes within the enriched B cell receptor signalling pathway, underscoring their significance in the biological processes related to rheumatoid arthritis

Table 4: Docking interaction scores for the Emodin and hub genes using CB-Dock2

CurPocket ID	*Vina score*	*Cavity volume (Å³)*	*Centre (x, y, z)*	*Docking size (x, y, z)*
Emodin-MET				
C1	-8.5	2845	9, 15, 141	31, 19, 19
C2	-6.3	348	20, 17, 157	19, 19, 19
C3	-6.2	287	0, 25, 158	19, 19, 19
C4	-6.2	251	29, 15, 118	19, 19, 19
C5	-5.6	222	10, 40, 152	19, 19, 19
Emodin-NFKB1				
C3	-7.1	278	9, -2, -13	19, 19, 19
C2	-6.4	342	21, 3, 13	19, 19, 19
C1	-5.9	792	14, -7, -5	19, 19, 19
C5	-5.6	133	24, 19, 1	19, 19, 19
C4	-4.9	246	21, 9, -7	19, 19, 19
Emodin-ABCG2				
C2	-8.1	6750	109, 109, 156	32, 29, 27
C3	-7.9	3120	109, 109, 73	19, 19, 32
C1	-7.7	7160	113, 109, 108	35, 35, 34
C5	-6.5	1020	94, 108, 126	19, 29, 35
C4	-6.2	1534	144, 112, 130	19, 19, 19

plex showed a Vina score of -7.1, with interactions involving residues ARG58, HIS66, and LEU142, further supporting its potential inhibitory effect (Fig. 6B). Similarly, the Emodin-ABCG2 complex exhibited a Vina score of -8.1 within a large cavity volume of 6750 Å³, interacting with residues across Chains A and B, including ASP296, THR213, and ARG246 (Fig. 6C). These interactions highlight emodin's potential as a multi-target inhibitor relevant to MET, NFKB1, and ABCG2, all of which are implicated in rheumatoid arthritis pathways.

MD Insights for Top Three Hub Genes

The MD simulations of the emodin-docked complexes with MET, NFKB1, and ABCG2, assessed using iMODS and CABS-flex, revealed differential stability and flexibility. The Emodin-MET complex demonstrated low deformity with stable B-factor values, and moderate RMSF values confirmed localised flexibility (Fig. 7A). The Emodin-NFKB1 complex exhibited higher flexibility than the other two, with moderate B-factor and RMSF values, indicating some instability near the binding site (Fig. 7B). In contrast, the Emodin-ABCG2 complex showed strong rigidity, with minimal deformity and low B-factor values, supported by low RMSF values, indicating a highly stable interaction (Fig. 7C). Overall, the simulations suggest that emodin forms stable interactions with MET and ABCG2, while exhibiting greater flexibility with NFKB1.

Expression Analysis of the Hub Genes

The differential gene expression analysis using the RABC134 dataset, comprising 689 samples (354 RA patients and 335 healthy controls), conducted via the RABC platform, revealed significant upregulation of three hub genes, namely, MET, NFKB1 and PARP1, in RA patients compared to healthy controls (Fig. 8A-E). These genes showed markedly higher expression levels, suggesting their potential involvement in RA pathogenesis. In contrast, the expressions of ABCG2 and ABCB1 were not statistically significant, indicating these genes may not be differentially expressed in the context of RA. These findings highlight the critical role of MET, NFKB1, and PARP1 in RA while suggesting a lesser involvement of ABCG2 and ABCB1.

R. Emodi Extract Induced Cytotoxicity

The CCK-8 assay demonstrated that the *R. emodi* extract induced a concentration-dependent reduction in the viability of SW-982 cells (Fig. 9A). Significant decreases in cell survival were observed at concentrations above 20/ µg/mL, with the IC_{50} estimated at 21.1/ µg/mL. These results indicate that the extract possesses potent cytotoxic activity, likely contributing to its anti-proliferative effects.

DAPI Staining Revealed Apoptotic Morphology

Microscopic examination of DAPI-stained cells showed distinct morphological changes in the IC50-

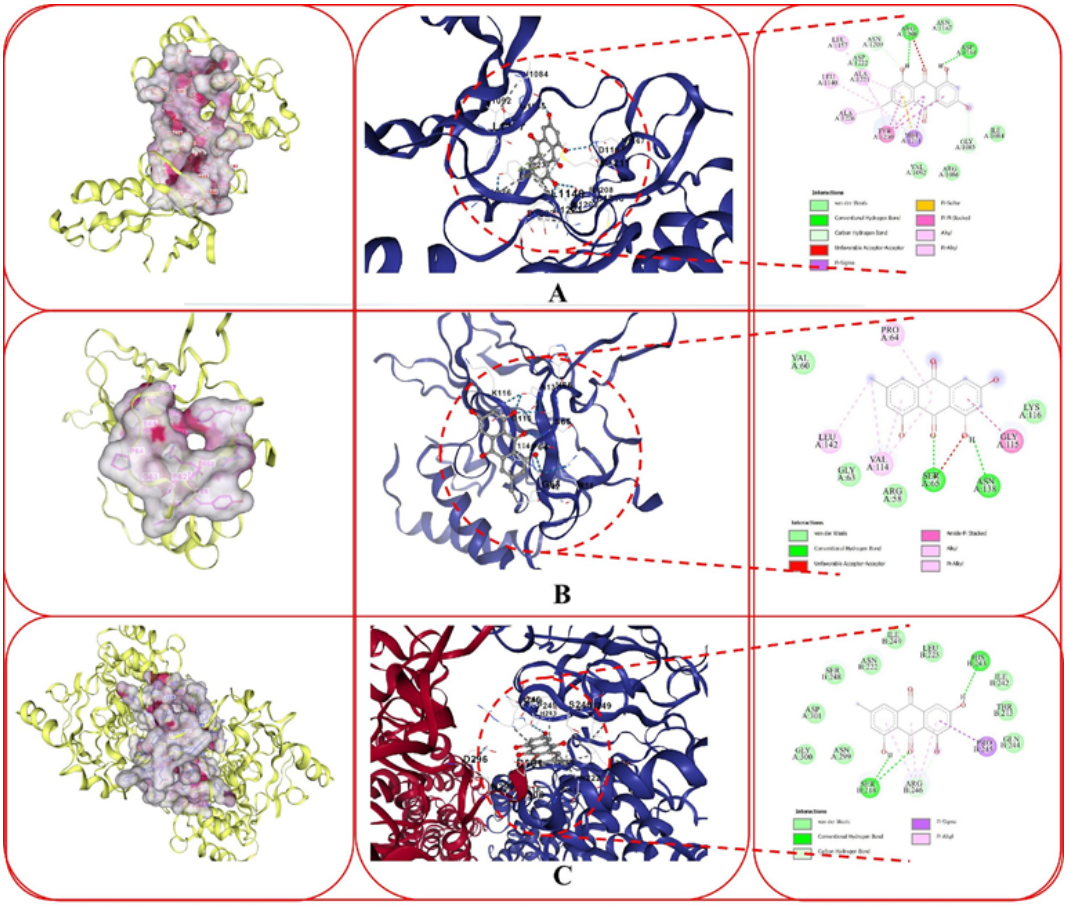

Fig. 6. (A) Molecular docking results for the Emodin-MET complex showing a Vina score of -8.5, indicating strong binding affinity, with key interactions identified with residues such as ILE1084, ARG1086, and MET1211 within a CurPocket of 2845 Å³
(B) Docking results for the Emodin-NFKB1 complex, which revealed a Vina score of -7.1 and significant interactions with residues ARG58, HIS66, and LEU142, suggesting its potential inhibitory effect on the target
(C) Molecular docking analysis for the Emodin-ABCG2 complex displaying a Vina score of -8.1 within a large cavity volume of 6750 Å³, with interactions noted across Chains A and B, including residues ASP296, THR213, and ARG246, emphasising emodin's potential as a multi-target inhibitor in rheumatoid arthritis pathways

treated group compared to control. Treated cells exhibited characteristic apoptotic features, including chromatin condensation and nuclear fragmentation, while control cells displayed uniform, intact nuclei (Fig. 9B). Representative images clearly demonstrated these qualitative differences, confirming the induction of apoptosis by the *Rheum emodi* extract.

DCFDA Assay Showed Increased ROS Production

Fluorescence microscopy revealed a noticeable increase in green fluorescence intensity in cells treated with the IC50 concentration of *Rheum emodi* extract compared to the control group. This qualitative observation indicated higher levels of

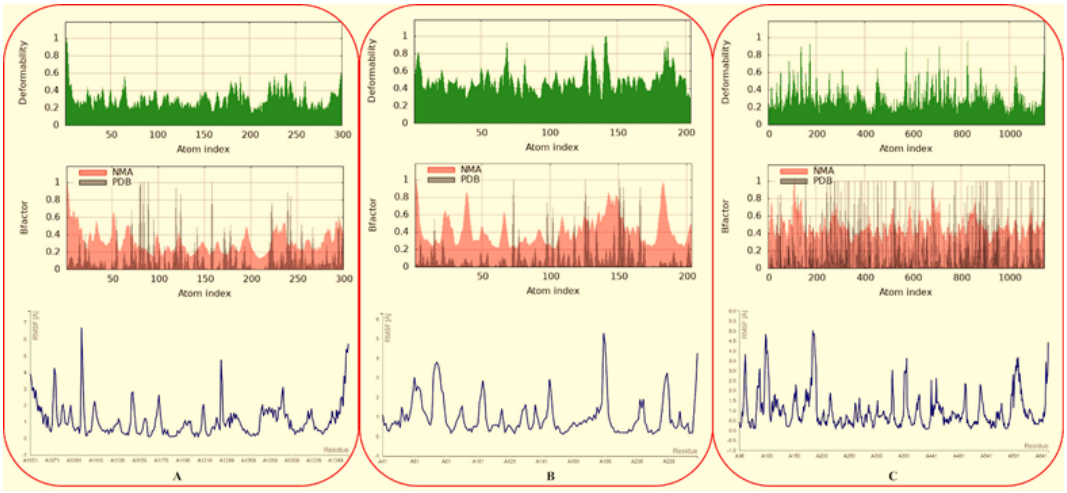

Fig. 7. (A) MD simulation results for the Emodin-MET complex indicating low deformity and stable B-factor values, suggesting a robust interaction profile. RMSF analysis of the Emodin-MET complex, showing moderate values that confirm localised flexibility in the binding region.
(B) B-factor analysis for the Emodin-NFKB1 complex, revealing moderate stability but indicating greater flexibility compared to the other complexes, particularly near the binding site. RMSF results for the Emodin-NFKB1 complex, demonstrating higher fluctuation values, which suggest some instability in the interaction
(C) B-factor results for the Emodin-ABCG2 complex, illustrating strong rigidity with minimal deformity, indicative of a highly stable interaction. RMSF analysis of the Emodin-ABCG2 complex showing low fluctuation values, confirming the stability of the interaction

ROS in treated cells (Fig. 10A). Representative images highlighted the contrast in fluorescence between the two groups, supporting the conclusion that the extract induces oxidative stress.

Scratch Assay Indicated Reduced Cell Migration

Visual assessment of the scratch assay over 24 hours demonstrated a clear delay in wound closure for the IC50-treated group compared to the control. Images taken at 24 hours showed minimal cell migration into the scratch area for treated cells, while control cells exhibited significant migration and wound closure (Fig. 10B). These qualitative observations suggested that the *Rheum Emodi* extract inhibits SW-082 cell migration.

Expression of Hub Genes in R. emodi Extract Treated SW-982 Cells

Gene expression analysis by qRT-PCR revealed that treatment with the extract significantly altered the transcriptional levels of key regulatory genes. Specifically, the expression of MET was markedly downregulated at IC50 concentration (21 µg/ml), suggesting an inhibition of proliferative signalling pathways (Fig. 11A). Concurrently, NFKB1 expression was reduced, indicating potential suppression of inflammatory and survival pathways (Fig. 11B). Additionally, ABCG2 levels were modulated, which may reflect alterations in cellular drug transport and resistance mechanisms (Fig. 11C). Together, these changes in gene expression corroborate the cytotoxic findings and suggest that the extract impacts multiple molecular targets involved in cell proliferation and survival.

DISCUSSION

The emergence of network pharmacology as a powerful framework in drug discovery facilitates a holistic understanding of the complex interactions between bioactive compounds and their molecular targets (Nogales et al. 2022). In this study, the

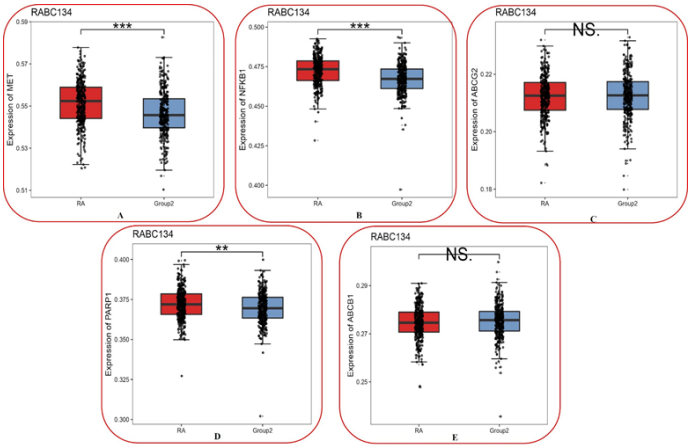

Fig. 8. Differential expression analysis results from the RABC134 dataset showing significant upregulation of hub genes MET, NFKB1, and PARP1 in rheumatoid arthritis patients compared to healthy controls, highlighting their potential role in RA pathogenesis

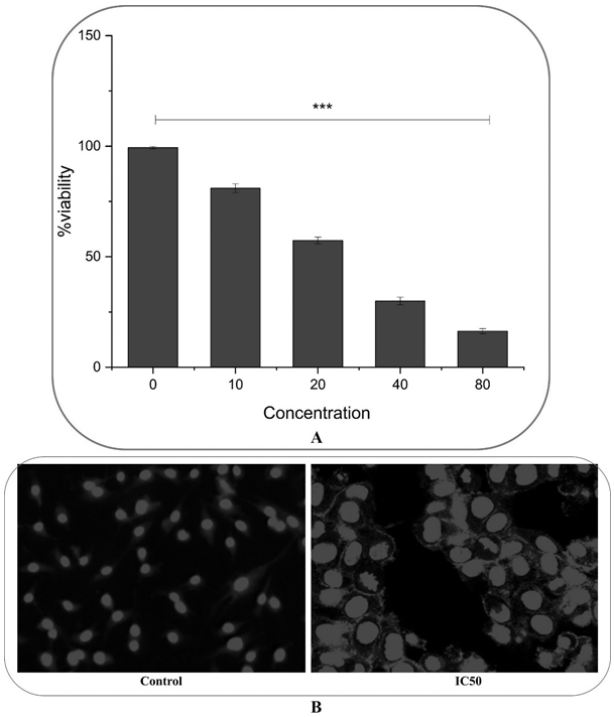

Fig. 9. *R. emodi* extract induces cytotoxicity and apoptosis in SW-982 cells
(A) CCK-8 assay showing a concentration-dependent decrease in cell viability, with an IC_{50} of 21.1 µg/mL
(B) DAPI staining of SW-982 cells treated with *Rheum emodi* extract (IC50). Control cells show uniform, intact nuclei (left panel), while treated cells exhibit apoptotic morphology including chromatin condensation and nuclear fragmentation (right panel)
Scale bar: 20 µm. (*p<0.001)**

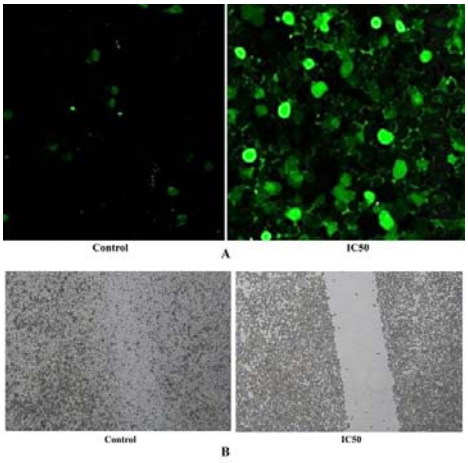

Fig. 10. (A) DCFDA assay for ROS detection in SW-982 cells. Fluorescence microscopy images show increased green fluorescence (ROS production) in cells treated with Rheum emodi extract (IC50, right panel) compared to control (left panel). Scale bar: 50 µm. (B) Scratch assay of SW-082 cell migration. Representative images at 24 hours post-scratch show delayed wound closure in Rheum emodi extract-treated cells (IC50, right panel) versus control (left panel)

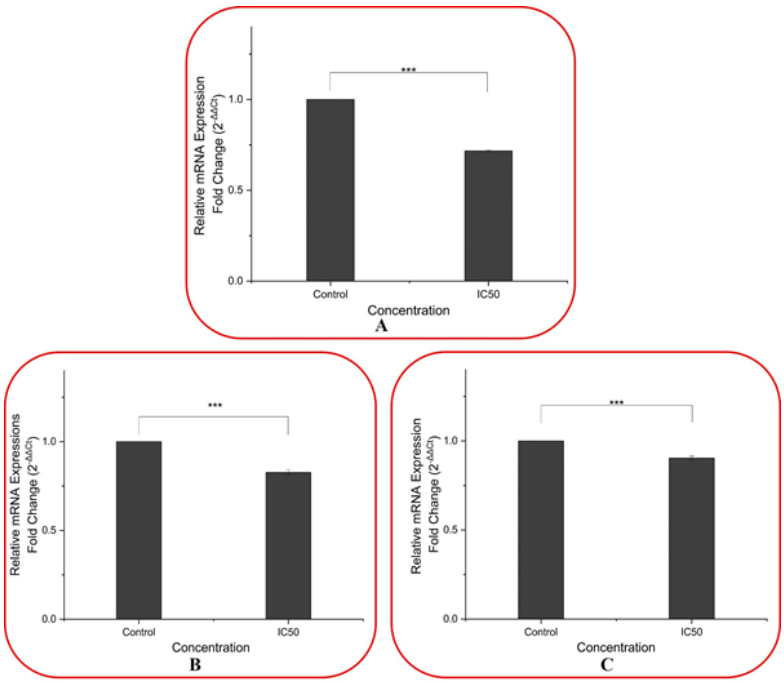

Fig. 11. qRT-PCR analysis of hub gene expression. (A) Downregulation of MET in treated cells (IC50: 21 µg/mL). (B) Reduced NFKB1 expression. (C) Modulated ABCG2 levels. Data normalized to control (dashed line). Error bars represent SEM (n=3). (*$p<0.001$)**

researchers explored the bioactive ingredients from *Rheum emodi* and their potential therapeutic roles in RA through an integrative approach involving molecular docking, dynamics simulations, gene ontology analysis, and differential expression studies. This multifaceted methodology not only identified key bioactive compounds but also elucidated their interaction networks, emphasising the importance of hub genes in RA pathology.

The screening process yielded six distinct bioactive compounds, each associated with multiple targets. Notably, the identification of 27 overlapping gene targets between the bioactive components of *Rheum emodi* and RA underscores the potential for these compounds to influence multiple pathways implicated in the disease. Among the targets, five hub genes, namely, *MET*, *NFKB1*, *ABCG2*, *PARP1*, and *ABCB1*, emerged as crucial components of the interaction network. These genes have been widely documented in the literature concerning RA, reinforcing their relevance in this context (Alhaddad et al. 2022; Qian et al. 2023).

MET, which encodes the hepatocyte growth factor receptor, plays a critical role in mediating cellular proliferation, survival, and differentiation (Hosonuma et al. 2021). In RA, aberrant activation of the *MET* signalling pathway is linked to enhanced inflammatory responses and joint destruction. Previous studies have demonstrated that targeting *MET* can mitigate synovial inflammation and bone erosion in RA models, supporting its potential as a therapeutic target (Nagashima et al. 2001). In this study, molecular docking results indicated strong binding affinity between emodin and *MET*, further validating its role as a therapeutic agent derived from *Rheum emodi*.

NFKB1 is another pivotal hub gene implicated in the regulation of inflammatory processes. Dysregulation of the NF-kB pathway is a hallmark of RA, contributing to the persistent inflammatory state observed in patients (Orozco et al. 2005). The docking results revealed favourable interactions between emodin and *NFKB1*, suggesting that this compound may modulate the inflammatory response through its action on this key signalling pathway. Additionally, gene ontology enrichment analysis identified biological processes related to cellular responses to chemical stimuli and lipid transport, which are critical in the pathogenesis of RA.

PARP1, involved in DNA repair and inflammatory signalling, has gained attention for its role in RA. Inhibition of *PARP1* has been shown to attenuate inflammation and joint damage in experimental models (Li et al. 2016). The differential expression analysis indicated significant upregulation of *PARP1* in RA patients compared to healthy controls, aligning with findings in the literature that suggest its potential as a therapeutic target in RA. *ABCG2* and *ABCB1*, both associated with drug transport and efflux mechanisms, presented contrasting results in this study, with no significant differential expression observed (Muto et al. 2021; Oerlemans et al. 2020). However, their role in pharmacokinetics cannot be overlooked, as they influence the absorption and efficacy of therapeutic agents.

Subsequent GO enrichment analysis revealed that the identified targets were significantly associated with biological processes such as lipid transport, cellular response to chemical stimuli, and regulation of cell differentiation. The KEGG analysis further elucidated pathways that may be implicated in RA, including the NF-kappa B signalling pathway, which is critical in inflammatory responses, and the ABC transporters pathway, known to play a role in drug resistance. These findings reinforce the hypothesis that *Rheum emodi* may exert its therapeutic effects through multiple mechanisms, targeting various pathways involved in the inflammatory process characteristic of RA. The molecular docking analysis provided insights into the binding affinities of the identified compounds with the key hub proteins. For instance, emodin demonstrated strong binding interactions with MET, NFKB1, and ABCG2, as indicated by Vina scores of -8.5, -7.1, and -8.1, respectively. These scores suggest that emodin has the potential to effectively inhibit these proteins, which are pivotal in RA. Molecular dynamics simulations further characterised the stability and flexibility of these docking complexes. The iMODS analysis revealed low deformity and stable B-factor values for the Emodin-MET and Emodin-ABCG2 complexes, indicating strong interactions, while the Emodin-NFKB1 complex exhibited higher flexibility, suggesting a more dynamic interaction. Finally, expression analysis using the RABC134 dataset provided valuable data on the differential expression of hub genes in RA versus healthy controls. The signifi-

cant upregulation of *MET*, *NFKB1*, and *PARP1* supports their critical roles in RA pathology, while the non-significant expression of *ABCG2* and *ABCB1* suggests that these genes may not be directly implicated in the disease process. This expression profile aligns with the findings from the PPI network, underscoring the potential of these hub genes as therapeutic targets for RA.

The findings suggest *Rheum emodi* extract exerts multifaceted effects on SW-082 cells. The observed apoptotic morphology and elevated ROS levels indicate potential cytotoxic activity, possibly through oxidative stress pathways. Reduced cell migration aligns with anti-metastatic properties, while downregulation of *MET* and *NFKB1* supports modulation of proliferative and inflammatory signalling. These qualitative outcomes, combined with network pharmacology predictions, highlight the extract's multi-target potential in targeting critical pathways. Further quantitative and mechanistic studies are warranted to validate these effects and explore therapeutic applications, particularly in conditions like RA where these pathways are dysregulated.

CONCLUSION

This study demonstrates that *Rheum emodi* extract exerts multifaceted effects on SW-982 cells, inducing apoptosis (DAPI), elevating ROS (DCFDA), and inhibiting migration (scratch assay), while qRT-PCR revealed downregulation of key genes (*MET*, *NFKB1*, *ABCG2*). These findings align with network pharmacology results identifying six bioactive compounds (for example, emodin, catechin) targeting 27 RA-associated genes, including five hub genes (*MET*, *NFKB1*, *ABCG2*, *PARP1*, *ABCB1*). Molecular docking confirmed emodin's strong binding to these targets, supported by GO/KEGG analyses linking them to NF-κB signalling and lipid transport. Expression data validated *MET*/*NFKB1*/*PARP1* upregulation in RA. Together, these results highlight *Rheum emodi*'s potential as a multi-target therapeutic agent, warranting further in vivo studies to translate these findings into RA treatment strategies.

RECOMMENDATIONS

To potentiate the pharmacotherapeutic utility of *Rheum emodi* in rheumatoid arthritis (RA), subsequent investigations should prioritise in vivo corroboration of emodin and allied bioactive moieties in preclinical animal models to substantiate efficacy, pharmacokinetic parameters, and toxicological profiles. Augmenting network pharmacology analyses with broader RA-associated signalling cascades and cross-referencing with disparate genomic repositories could refine target specificity. Prolonged molecular dynamics simulations should interrogate conformational stability and intermolecular interactions under physiological milieu. In vitro assays should integrate primary RA synovial fibroblasts to emulate pathophysiologic contexts. Furthermore, early-phase clinical trials are imperative to evaluate *R. emodi* extract's therapeutic efficacy, optimal pharmacodynamic dosing, and potential adverse effects in RA cohorts, ensuring translational fidelity.

CONFLICT OF INTEREST

None.

ACKNOWLEDGEMENTS

None.

AUTHOR CONTRIBUTIONS

X.N. and Y.F. contributed equally to this study. Both authors were involved in the conception and design of the research, performed the computational and experimental analyses, interpreted the data, and contributed to drafting and revising the manuscript. Both the authors have read and approved the final version of the manuscript and agree to be accountable for all aspects of the work.

FUNDING STATEMENT

None.

REFERENCES

Alhaddad L, Osipov AN, Leonov S 2022. The molecular and cellular strategies of glioblastoma and non-small-cell lung cancer cells conferring radioresistance. *Int J Mol Sci*, 23(21): 13577.

AlRawashdeh S, Barakat KH 2023. Applications of molecular dynamics simulations in drug discovery. *Comput Drug Discov Des*, 127-141.

Chen P, Dai Z, Ye S 2025. Network pharmacology based in silico and in vitro anticancer effects of Artemisia maritima extract in human prostate cancer cells. *Iran J Chem Chem Eng*, 44(4): 991-1008.

Daina A, Michielin O, Zoete V 2017. SwissADME: A free web tool to evaluate pharmacokinetics, drug-likeness and medicinal chemistry friendliness of small molecules. *Sci Rep*, 7(1): 42717.

Daina A, Michielin O, Zoete V 2019. SwissTargetPrediction: Updated data and new features for efficient prediction of protein targets of small molecules. *Nucleic Acids Res*, 47(W1): W357-364.

Finckh A, Gilbert B, Hodkinson B, Bae SC, Thomas R, Deane KD, Alpizar-Rodriguez D, Lauper K 2022. Global epidemiology of rheumatoid arthritis. *Nat Rev Rheumatol*, 18(10): 591-602.

Gadzhanova S, Roughead E 2024. Use of analgesic and anti inflammatory medicines before and after initiation of biological disease modifying antirheumatic drugs for rheumatoid arthritis. *J Clin Pharm Ther*, 2024(1): 8040681.

Hosonuma M, Sakai N, Furuya H, Kurotaki Y, Sato Y, Handa K, Dodo Y, Ishikawa K, Tsubokura Y, Negishi-Koga T, Tsuji M 2021. Inhibition of hepatocyte growth factor/c-Met signalling abrogates joint destruction by suppressing monocyte migration in rheumatoid arthritis. *Rheumatology*, 60(1): 408-419.

Jiang C, Liu Y, Xu H 2025. Network-pharmacology-based mechanism elucidation and validation for phytochemicals from Artemisia Vestita against osteoarthritis. *Iran J Chem Chem Eng*, 44(3): 687-706.

Kondo N, Kuroda T, Kobayashi D 2021. Cytokine networks in the pathogenesis of rheumatoid arthritis. *Int J Mol Sci*, 22(20): 10922.

Kuriata A, Gierut AM, Oleniecki T, Ciemny MP, Kolinski A, Kurcinski M, Kmiecik S 2018. CABS-flex 2.0: A web server for fast simulations of flexibility of protein structures. *Nucleic Acids Res*, 46(W1): W338-343.

Li G, Cunin P, Wu D, Diogo D, Yang Y, Okada Y, Plenge RM, Nigrovic PA 2016. The rheumatoid arthritis risk variant CCR6DNP regulates CCR6 via PARP-1. *PLoS Genet*, 12(9): e1006292.

López-Blanco JR, Aliaga JI, Quintana-Ortí ES, Chacón P 2014. iMODS: Internal coordinates normal mode analysis server. *Nucleic Acids Res*, 42(W1): W271-276.

Makuch S, Wiêcek K, WoIniak M 2021. The immunomodulatory and anti-inflammatory effect of curcumin on immune cell populations, cytokines, and in vivo models of rheumatoid arthritis. *Pharmaceuticals*, 14(4): 309.

Muto S, Minamitani N, Ogura T, Nakajima A, Nakagawa K, Masaka T, Hiura S, Kobayashi H, Kato H, Kameda H 2021. Good response to methotrexate is associated with a decrease in the gene expression of ABCG2, a drug transporter, in patients with rheumatoid arthritis. *Mod Rheumatol*, 31(6): 1079-1086.

Nagashima MA, Hasegawa J, Kato K, Yamazaki JU, Nishigai KE, Ishiwata TO, Asano GO, Yoshino SH 2001. Hepatocyte growth factor (HGF), HGF activator, and c-Met in synovial tissues in rheumatoid arthritis and osteoarthritis. *J Rheumatol*, 28(8): 1772-1778.

Nogales C, Mamdouh ZM, List M, Kiel C, Casas AI, Schmidt HH 2022. Network pharmacology: Curing causal mechanisms instead of treating symptoms. *Trends Pharmacol Sci*, 43(2): 136-150.

Oerlemans R, Blits M, Dijkmans BA, van der Heijden JW, Lems WF, Scheffer GL, van de Ven R, Peters GJ, Assaraf YG, Scheper RJ, Jansen G 2020. Expression profiling of ABC transporters in peripheral blood lymphocytes and monocyte-derived macrophages of rheumatoid arthritis patients. *J Mol Clin Med*, 3(2): 47-60.

Orozco G, Sanchez E, Collado MD, Lopez Nevot MA, Paco L, Garcia A, Jiménez Alonso J, Martín J 2005. Analysis of the functional NFKB1 promoter polymorphism in rheumatoid arthritis and systemic lupus erythematosus. *Tissue Antigens*, 65(2): 183-186.

Patel L, Shukla T, Huang X, Ussery DW, Wang S 2020. Machine learning methods in drug discovery. *Molecules*, 25(22): 5277.

Qian H, Jin Q, Liu Y, Wang N, Chu Y, Liu B, Liu Y, Jiang W, Song Y 2023. Study on the multitarget mechanism of Sanmiao Pill on gouty arthritis based on network pharmacology. *Evid Based Complement Alternat Med*, 6(14): 476-489.

Rolta R, Salaria D, Kumar V, Patel CN, Sourirajan A, Baumler DJ, Dev K 2022. Molecular docking studies of phytocompounds of Rheum emodi Wall with proteins responsible for antibiotic resistance in bacterial and fungal pathogens: In silico approach to enhance the bio-availability of antibiotics. *J Biomol Struct Dyn*, 40(8): 3789-3803.

Shen Y, Teng L, Qu Y, Liu J, Zhu X, Chen S, Yang L, Huang Y, Song Q, Fu Q 2022. Anti-proliferation and anti-inflammation effects of corilagin in rheumatoid arthritis by downregulating NF-κB and MAPK signaling pathways. *J Ethnopharmacol*, 284: 114791.

Shinbo Y, Nakamura Y, Altaf-Ul-Amin M, Asahi H, Kurokawa K, Arita M, Saito K, Ohta D, Shibata D, Kanaya S 2006. KNApSAcK: A comprehensive species-metabolite relationship database. *Plant Metabolomics*, 2006: 165-181.

Singh S, Singh TG, Mahajan K, Dhiman S 2020. Medicinal plants used against various inflammatory biomarkers for the management of rheumatoid arthritis. *J Pharm Pharmacol*, 72(10): 1306-1327.

Stanzione F, Giangreco I, Cole JC 2021. Use of molecular docking computational tools in drug discovery. *Prog Med Chem*, 60: 273-343.

Stelzer G, Rosen N, Plaschkes I, Zimmerman S, Twik M, Fishilevich S, Stein TI, Nudel R, Lieder I, Mazor Y, Kaplan S 2016. The GeneCards suite: From gene data mining to disease genome sequence analyses. *Curr Protoc Bioinformatics*, 54(1): 1-30.

Szklarczyk D, Gable AL, Nastou KC, Lyon D, Kirsch R, Pyysalo S, Doncheva NT, Legeay M, Fang T, Bork P, Jensen LJ 2021. The STRING database in 2021: Customizable protein–protein networks, and functional characterization of user-uploaded gene/measurement sets. *Nucleic Acids Res*, 49(D1): D605-612.

Vivek-Ananth RP, Mohanraj K, Sahoo AK, Samal A 2023. IMPPAT 2.0: An enhanced and expanded phytochemical atlas of Indian medicinal plants. *ACS Omega*, 8(9): 8827-8845.

Weyand CM, Goronzy JJ 2021. The immunology of rheumatoid arthritis. *Nat Immunol*, 22(1): 10-18.

Zhang X, Nan H, Guo J, Liu J 2021. NLRP12 reduces proliferation and inflammation of rheumatoid arthritis fibroblast-like synoviocytes by regulating the NF-êB and MAPK pathways. *Eur Cytokine Netw*, 32(2): 15-22.

Zhou J, Chen Y, Zeng X, Gong F, Zhang X 2025. Investigating anticancer properties of Artemisia annua in human pancreatic cancer cells: Insights from network pharmacology, molecular docking, dynamics simulations, and experimental testing. *Iran J Chem Chem Eng*, 44(3): 666-686.

Paper received for publication in August, 2025
Paper accepted for publication in October, 2025